Journal of Applied Electrochemistry **29**: 1119–1123, 1999.

Zinc dissolution in ammonium chloride electrolytes

A.B. VELICHENKO[1], J. PORTILLO[2], M. SARRET[1] and C. MULLER[1]*
[1]*LCTEM. Department of Physical Chemistry, University of Barcelona, Martí i Franqués 1, 08028 Barcelona, Spain;*
[2]*Serveis Científico-Técnics, University of Barcelona, Spain*
*(*author for correspondence)*

Received 7 October 1998; accepted in revised form 2 March 1999

Key words: anodic dissolution, XPS, zinc, zinc hydroxide film

Abstract

The anodic dissolution of zinc RDE in NH_4Cl and $NH_4Cl + ZnCl_2$ electrolytes at pH 5.5 was studied. XPS and SEM data indicate that the zinc electrode is covered by a porous film composed of a mixture of metallic zinc and zinc hydroxide. The thickness of the film and the zinc hydroxide content is much higher in zinc-containing electrolytes than in NH_4Cl and, although the thickness and $Zn(OH)_2$ amount decrease with anodic polarization, the electrode is never free from oxidized compounds. Electrochemical results indicate that at low overpotentials the rate of zinc dissolution is determined by the removal of the oxidized blocking particles, while at high overpotentials Zn dissolution takes place through the porous layer.

1. Introduction

The behaviour of the zinc anode plays a critical role in Zn–Ni electroplating since the passivation of the anode increases the potential difference between the electrodes and reduces the coating quality. In a previous study on Ni-containing ammonium electrolytes [1] it was observed that, with external anodic current, passive film formation was a result of space-sharing anodic and cathodic reactions due to local Ni or Zn–Ni alloy electrodeposition. XPS results indicated that metallic Zn, metallic Ni or Ni–Zn alloy and zinc-oxygen-containing compounds (ZnO_xH_y) were present in this passive film, which was probably a product of the Zn dissolution reaction.

Two possible explanations can be advanced to account for the incorporation of the oxygen-containing particles into the passive film. The first is chemical precipitation, particularly in conditions of hydrogen evolution on Ni-rich surfaces. At pH > 5, zinc hydroxide can precipitate to form $Zn(OH)_2.ZnO$ [2] or $ZnCl_2.4Zn(OH)_2$ [3] films. The second is electrochemical formation due to the anodic dissolution of the zinc electrode. Baugh [4] suggested that in NH_4Cl solutions the anode surface is free from oxygen-containing particles. In other cases, however, an oxide layer appears at low anodic polarizations which is subsequently removed at high current densities [5].

The kinetics of the zinc dissolution reaction in NH_4Cl solutions has been extensively investigated using polarization measurements and impedance techniques [4–8]. The reaction is strongly stimulated by chloride anions, which appear to be responsible for zinc corrosion. In alkaline solutions, where the oxide film formation is ensured, significant changes in the kinetics of zinc dissolution are observed [9]. Metal dissolution takes place essentially at the base of pores of a conductive layer of oxidation products which is progressively degraded by the anodic current.

The main aim of this study was to obtain more information on the zinc dissolution process and on the nature of the anodic film formed on Zn electrode in NH_4Cl and $NH_4Cl + ZnCl_2$ solutions using electrochemical and surface analysis techniques. The results obtained will be useful as a reference, prior to the analysis of anode behaviour in the industrial electrolytes used to obtain Zn–Ni alloys.

2. Experimental details

Electrochemical measurements were carried out in a three-electrode cell of 0.1 dm^3 capacity. NH_4Cl and $NH_4Cl + ZnCl_2$ solutions with fixed Cl^- concentration (3 mol dm^{-3}) at pH 5.5 were used. All chemicals were Merck pro-analysis grade and the water was obtained from MilliQ water purification system. The electrolytes were deoxygenated by argon bubbling before and during use. The temperature of the solutions was 25 °C in all cases. All potentials are given against Ag/AgCl/KCl (sat.) electrode. The zinc disc electrode (diameter 2 mm) was mounted in a Teflon holder which was connected to a Taccussel CTV101T rotator. Before each measurement the zinc electrode was polished with silicon carbide paper (grade 1000 and

4000) and aluminum oxide (3.75 μm), etched with 1:10 HCl:H_2O solution for 2 min and rinsed in doubly distilled water. The electrochemical measurements were performed after reaching the steady-state potential using an EG&G 273 potentiostat controlled by a 486 IBM PC. Ohmic drop was corrected by using the current-interrupt IR compensation method. The film morphology and surface chemical analysis were examined by scanning electron microscopy (SEM) and X-ray photoelectron spectroscopy (XPS).

3. Results and discussion

3.1. *Electrochemical data*

The electrochemical study of zinc anodic dissolution was mainly performed using cyclic voltammetry and quasi steady-state i/E curves ($v = 1\,\mathrm{mV\,s^{-1}}$). Given the strong influence of the chloride ion content on this process [5], all data were obtained with a constant Cl^- concentration (3 mol dm^{-3}). It was observed that a change in NH_4^+ concentration in the range 1–3 mol dm^{-3} hardly influenced the i/E curves, at a constant Cl^- content.

Typical i/E curves for the supporting electrolyte and different zinc-containing solutions are shown in Figure 1. The dependence of the anodic current on the electrode rotation speed indicates that the rate of zinc dissolution is determined by a diffusion stage, probably the rate at which zinc-chloro species diffuse away from the electrode [5, 6]. However, at rotation speeds over 1000 rpm the current becomes independent of the rotation speed, which indicates that there is no diffusion control in the bulk electrolyte.

Cyclic voltammograms for the zinc electrode at $\omega = 2000$ rpm are shown in Figure 2(a). Differences in the current for forward and reverse scans are observed, depending on the potential scan rate (v). These differences decrease with decreasing potential scan rate and disappear at high overpotentials for $v \leq 1\,\mathrm{mV\,s^{-1}}$. The dependence of the current density on the potential scan rate is shown in Figure 2(b). It is relevant that the current decreases as the scan rate increases. These voltammetric results indicate that zinc dissolution depends not just on potential, but also on time.

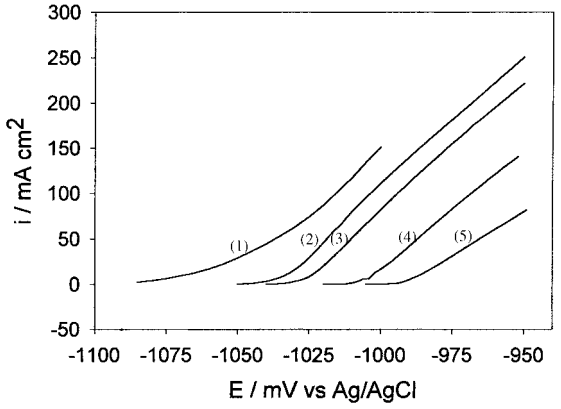

Fig. 1. Polarization curves for Zn RDE at $\omega = 2000$ rpm in different solutions: (1) 3.0 mol dm^{-3} NH_4Cl; (2) 2.8 mol dm^{-3} NH_4Cl + 0.1 mol dm^{-3} $ZnCl_2$; (3) 2.5 mol dm^{-3} NH_4Cl + 0.25 mol dm^{-3} $ZnCl_2$; (4) 2.0 mol dm^{-3} NH_4Cl + 0.5 mol dm^{-3} $ZnCl_2$; (5) 1.0 mol dm^{-3} NH_4Cl + 1.0 mol dm^{-3} $ZnCl_2$. $v = 1\,\mathrm{mV\,s^{-1}}$.

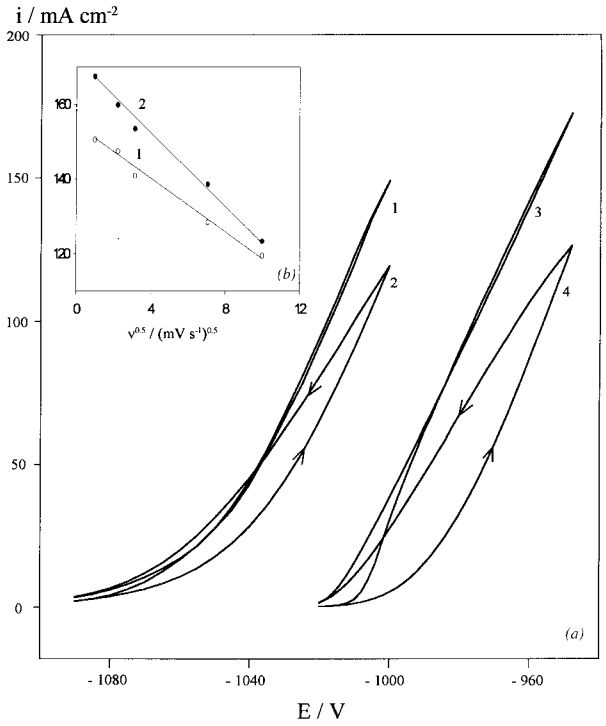

Fig. 2. (a) Cyclic voltammograms for Zn RDE at $\omega = 2000$ rpm in 3.0 mol dm^{-3} NH_4Cl (1, 2) and 2.0 mol dm^{-3} NH_4Cl + 0.5 mol dm^{-3} $ZnCl_2$ (3, 4) at different potential scan rates: (1, 3) –2 mV s^{-1}; (2, 4) –100 mV s^{-1}. (b) Dependence of anodic current density on potential scan rate for Zn RDE at $\omega = 2000$ rpm in different solutions: (1) 3.0 mol dm^{-3} NH_4Cl, $E = -1.000$ V; (2) 2.0 mol dm^{-3} NH_4Cl + 0.5 mol dm^{-3} $ZnCl_2$, $E = -0.950$ V.

The kinetics of zinc dissolution was analyzed using quasi steady-state i/E curves ($v = 1\,\mathrm{mV\,s^{-1}}$) at $\omega =$ 2000 rpm. The method proposed by Shub in [10] was used to calculate the electrode resistance (R) and to correct i/E curves for IR drop. This method has been used successfully in other cases to calculate the electrode resistance and Tafel slopes in complex anodic processes [11, 12]. In the present study it was found that the experimental and calculated polarization curves corrected for ohmic drop showed the same trends (Figure 3(a)). Shub suggests that the experimental polarization curves (PC) may reflect three situations:

(i) The character of the PC at high i is controlled by ohmic drop.

(ii) The character of the PC at high i is determined, not only by ohmic drop, but also by special kinetic features of the anodic reaction.

(iii) The character of the PC at high i is determined both by ohmic drop and by special kinetic features, but the electrode resistance changes. In this case two linear sections occur on dE against i plots (dE is the

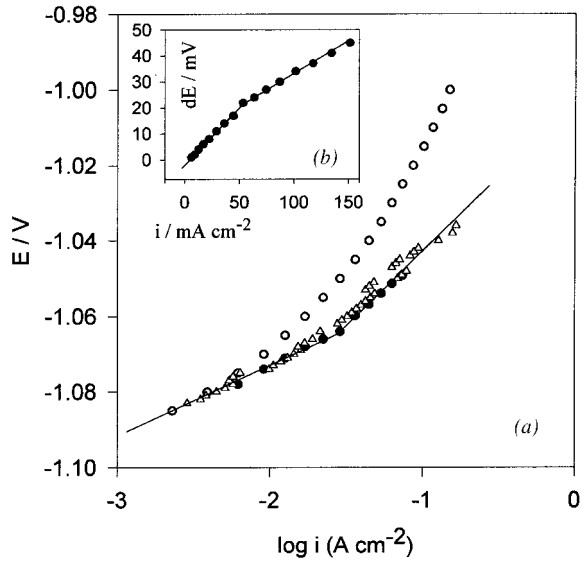

Fig. 3. (a) Anodic polarization curves for Zn RDE at $\omega = 2000$ in 3.0 mol dm^{-3} NH_4Cl: (○) experimental, uncorrected for ohmic drop; (△) experimental, corrected for ohmic drop; (●) calculated, corrected for ohmic drop; (b) dE against i plot corresponding to the experimental uncorrected curve.

difference between the experimental potential and the potential obtained by the extrapolation of the initial linear segment of the CP) [12]. R_1 is calculated directly from the slope of the first section (at low i) and R_2 is calculated from equation [10]:

$$R = R_0 - \mathrm{d}E_0(\log i_2 - \log i_1) \times [(i_2 \log i_1 - i_1 \log i_2) - (i_2 - i_1)\log i_x] \quad (1)$$

where R_0 is the resistance calculated from the slope of 2nd section of dE against i plots; dE_0 is the value obtained when this section is extrapolated to the axis of dE; i_1 and i_2 are relatively high current densities found within the 2nd section ($i_2 \leqslant 1.5\, i_1$); and i_x is the current density of intersection on dE against i plots.

The polarization curve obtained with the supporting electrolyte and dE against i plot are shown in Figures 3(a) and (b), respectively. According to Figure 3(b) the resistance of the electrode changes with potential, with $R_1 = 0.50 \pm 0.05\ \Omega$ at low overpotentials ($E < -1.060$ V) and $R_2 = 0.31 \pm 0.05\ \Omega$ at high overpotentials ($E > -1.060$ V). These resistance values are used to simulate the true polarization curve (Figure 3(a)), for which two Tafel slopes are obtained: $b_1 = 20$ mV per decade at low overpotentials and $b_2 = 26$ mV per decade at high overpotentials. As also observed in Figure 3(a), the PC with the ohmic drop experimentally corrected shows the same slopes. However, only one Tafel slope is observed in the reverse scan of the i/E curves and this is close to the value of $2.3RT/2F$, which, according to [4], corresponds to a reversible zinc dissolution process.

When Zn is present in the electrolyte, a shift of polarization curves to positive potentials is observed (Figure 1) due to changes in the equilibrium potential of the Zn electrode. The analysis of the quasi steady-state i/E curves (performed using the same method) for the solution 2 mol dm^{-3} NH_4Cl + 0.5 mol dm^{-3} $ZnCl_2$ also shows different Tafel slopes. In the forward scan, slopes of $b_1 = 8$ mV per decade at low overpotentials ($E < -1.010$ V) and $b_2 = 28$ mV per decade at high overpotentials ($E > -1.010$ V) are calculated. As observed with the supporting electrolyte, at high overpotentials the current for the forward and for the reverse scans of the quasi steady-state i/E curve is the same and Tafel slope b_2 indicates a reversible zinc dissolution process [4]. However, at low overpotentials the current on the reverse scan of the polarization curves changes more quickly and a Tafel slope of 10 mV per decade (b_1) is calculated. Moreover, the resistance of the electrode practically does not change with increasing potential: at low overpotentials $R_1 = 0.32 \pm 0.05\ \Omega$ and $R_2 = 0.36 \pm 0.05\ \Omega$ at high overpotentials.

3.2. *Surface analysis data*

To analyse the nature of the film formed on the zinc anode surface after anodic polarization in the supporting electrolyte and in 2 mol dm^{-3} NH_4Cl + 0.5 mol dm^{-3} $ZnCl_2$ solution, SEM and XPS techniques were used. A porous film is observed in both cases (Figure 4), but, in the presence of zinc large amorphous blocks are formed on the electrode surface. This

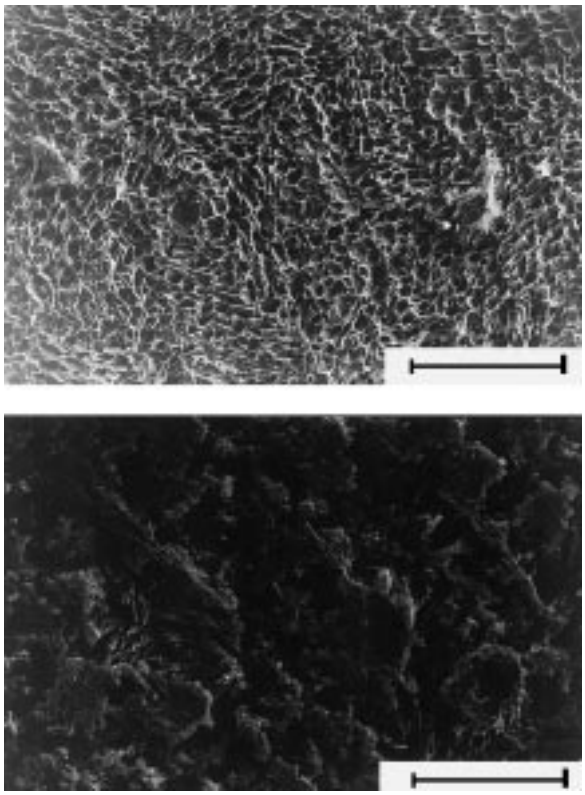

Fig. 4. SEM micrographs of film on zinc RDE prepared at $\omega =$ 500 rpm. for 10 min in: (1) 3.0 mol dm^{-3} NH_4Cl ($E = -1.000$ V); (2) 2.0 mol dm^{-3} NH_4Cl + 0.5 mol dm^{-3} $ZnCl_2$ ($E = -0.940$ V). Scalebars: 100 μm.

indicates that the formation of insoluble products on the zinc electrode surface is favoured in the zinc-containing solutions.

XPS results indicate that in both cases the film formed on the zinc anode contains only two elements: zinc and oxygen. Nitrogen and chlorine are not detected either on the surface or in the bulk of the film. The nature of the oxygen-containing compounds is determined by analysing the XPS peak position of oxygen and zinc. As a reference material we used ZnO which was pressed into a tablet as a mixture of ZnO + KBr. By taking the C1s peak from contamination at a binding energy (BE) of 284.8 eV, the BE of O1s of ZnO was found at 530.4 eV. This value was consistent with published data [13]. The binding energy of Br3d (69.0 eV) was used to correct peak position [14] and then, the BE of O1s after sputtering was found at 529.7 eV. Given that there was practically no difference between the BE of $Zn2p_{3/2}$ in metallic and oxidized forms [13, 14], we obtained the Zn LMM Auger line for the ZnO sample. In this case the kinetic energy (KE) value for Zn^{2+} in ZnO (989.1 eV) was quite different from the KE of Zn^0 in the metal (992.2 eV). Thus, the Zn LMM Auger line was used for the analysis of the film.

The LMM lines of Zn for a pure Zn metallic foil, ZnO and a zinc anode after anodic polarization are shown in Figure 5. It should be noted that the peak position obtained for zinc anodes oxidized in the supporting electrolyte or in the 2 mol dm^{-3} $NH_4Cl + 0.5$ mol dm^{-3} $ZnCl_2$ solution is the same. Comparison of these spectra demonstrates that the anodic film on the Zn electrode is a mixture of metallic zinc and zinc–oxygen compounds. Based on the peak positions of Zn^{2+} LMM (KE = 987.2 eV) and O1s (BE in range 532.0–531.5 eV), the majority of Zn(II) is in the $Zn(OH)_2$ form.

According to XPS depth profiles (Figure 6), the content of $Zn(OH)_2$ in the film formed in the presence of zinc is much higher than that obtained with the supporting solution: in both cases this content decreases with film depth. Moreover, the amount of $Zn(OH)_2$ and the film thickness depend on the applied potential (current density) and on time for film formation. They decrease with increasing overpotential and decreasing formation time.

Therefore, XPS results indicate that the film formed on the zinc anode surface in ammonium electrolytes contains zinc hydroxide, even at high overpotentials, which is contrary to what was suggested in other cases [4, 5]. The formation of a porous layer of zinc and $Zn(OH)_2$ on the zinc electrode close to the equilibrium potential may account for the electrochemical results: with this layer, electrode activation (the removing of some blocking particles, mainly $Zn(OH)_2$) is necessary for the current to flow through the electrode, which explains why the current is higher at low scan rates or a Tafel slope lower than the 'reversible' value. However, this film is non-blocking, probably because it is a thin film with metallic conductivity and porous structure [9] and so zinc oxidation can take place to some extent

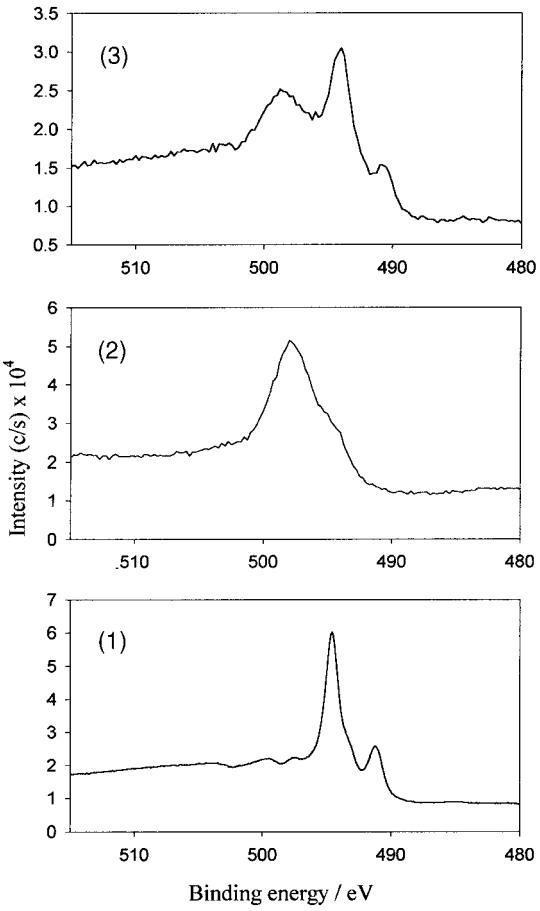

Fig. 5. XPS spectra in the Zn LLM region for: (1) Zn foil; (2) ZnO pressed into a tablet with KBr; (3) film formed on the Zn anode in 2.0 mol dm^{-3} $NH_4Cl + 0.5$ mol dm^{-3} $ZnCl_2$ ($E = -0.940$ V, $\omega =$ 500 rpm.) for 10 min.

through the film. With polarization some of the $Zn(OH)_2$ particles that hinder the oxidation of zinc are removed and at high anodic overpotentials the Tafel slope attains the reversible value, although the electrode is not free of oxidized compounds. Since $Zn(OH)_2$ has low conductivity, the resistance of the electrode decreases with polarization. The behaviour in the reverse scans

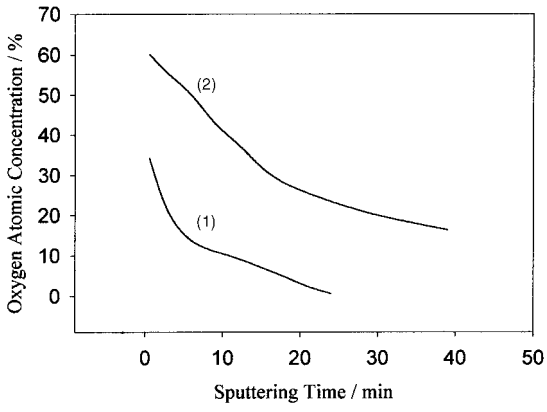

Fig. 6. O1s XPS depth profile for film on zinc RDE prepared at $\omega = 500$ rpm. for 10 min in: (1) 3.0 mol dm^{-3} NH_4Cl ($E = -1.000$ V); (2) 2.0 mol dm^{-3} $NH_4Cl + 0.5$ mol dm^{-3} $ZnCl_2$ ($E = -0.940$ V).

of the i/E curves indicates that the electrode surface is free from the blocking particles that are removed from the surface at low overpotentials in the forward scan.

In zinc-containing electrolytes film thickness increases and is richer in zinc hydroxide. Given the thickness and composition of the layer it seems that in this case zinc oxidation can only take place if some of the blocking particles are previously removed from the surface. If this occurs, the effective anode area increases, the current increases abruptly and a very low Tafel slope is obtained. Moreover, in these conditions the resistance of the electrode is constant, maintaining the same value when it is obtained at high overpotentials with the supporting electrolyte. This indicates that this value corresponds to the zinc anode when it is free from the oxidized compounds that hinder the oxidation process. The low value of the Tafel slope for the reverse scan of the PC at low overpotentials indicates that the blocking particles are also formed at low anodic overpotentials, probably because oxygen-containing species can form more easily when Zn^{2+} is present in the solution.

4. Conclusions

XPS analysis of zinc dissolution in ammonium chloride electrolytes indicates that the zinc surface is covered by a porous layer, composed of metallic zinc and zinc hydroxide, formed at the corrosion potential. The thickness of this layer and the amount of zinc hydroxide is much higher in $NH_4Cl + ZnCl_2$ than in NH_4Cl electrolytes and, although the thickness decreases with overpotential, the surface is never completely free of oxidation products.

Electrochemical results indicate that, at low overpotentials, the rate of zinc dissolution is determined by the removal of some of the $Zn(OH)_2$ particles that block the electrode surface. At high overpotentials Zn dissolution takes place through the porous layer that remains on the surface.

Acknowledgements

The authors are grateful to the CICYT (project number MAT 97-0379) for financial assistance and to the Serveis Científico-Tècnics of the Universitat de Barcelona for SEM and surface analysis measurements. We also thank the Generalitat de Catalunya for the financial support of A.B.V.

References

1. A.B. Velichenko, M. Sarret and C. Muller, *J. Electroanal. Chem.* **448** (1998) 1.
2. D.R. Gabe, *in* 'Oxides and Oxide Film'. Vol. 6 (Marcel Dekker, New York, 1981), ed. J.W. Diggle, pp. 203.
3. V. Ravindran and V.S. Muralidharan, *Trans. SAEST* **26** (1991) 193.
4. L.M. Baugh, *Electrochim. Acta* **24** (1979) 669.
5. C. Cachet and R. Wiart, *J. Electroanal. Chem.* **111** (1980) 235.
6. C. Cachet and R. Wiart, *J. Electroanal. Chem.* **129** (1981) 103.
7. M. Maja, N. Penazzi, G. Farnia and G. Sandona, *Electrochim. Acta* **38** (1993) 1453.
8. V. Ravindran and V.S. Muralidharan, *Bull. Electrochem.* **6(2)** (1990) 237.
9. C. Cachet, B. Saidani and R. Wiart, *J. Electrochem. Soc.* **139** (1992) 644.
10. D.M. Shub, M.F. Reznik and V.V. Shalaginov, *Electrokhimiya* **21** (1985) 878.
11. D.M. Shub and M.F. Reznik, *Electrokhimiya* **21** (1985) 795.
12. F.I. Danilov, A.B. Velichenko, S.M. Loboda and R.L. Mokienko, *Electrokhimiya* **25** (1989) 406.
13. B. Matel, A. Ben Taleb, O. Dessaux, P. Goudmand, L. Gengembre and J. Grimblot, *Thin Solid Films* **266** (1995) 119.
14. J.F. Moulder, W.F. Stickle, P.E. Sobol and K.D. Bomben, Handbook of X-ray Photoelectron Spectroscopy, 2nd edn, (Physical Electronics: Eden Prairie, Minnesota 1995).